Nuclear Instruments and Methods in Physics Research A 712 (2013) 34–40

Contents lists available at SciVerse ScienceDirect

Nuclear Instruments and Methods in Physics Research A

journal homepage: www.elsevier.com/locate/nima

Performance of cerium-doped $Gd_3Al_2Ga_3O_{12}$ (GAGG:Ce) scintillator in gamma-ray spectrometry

Joanna Iwanowska [a,*], Lukasz Swiderski [a], Tomasz Szczesniak [a], Pawel Sibczynski [a], Marek Moszynski [a], Martyna Grodzicka [a], Kei Kamada [b], Kousuke Tsutsumi [b], Yoshiyuki Usuki [b], Takayuki Yanagida [c], Akira Yoshikawa [c]

[a] National Centre for Nuclear Research, 05-400 Otwock/Swierk, Poland
[b] Furukawa Company Ltd., Tsukuba, 305-0856 Ibaraki, Japan
[c] IMRAM, Tohoku University, Aoba-ku, Sendai, 980-8577 Miyagi, Japan

ARTICLE INFO

Article history:
Received 11 July 2012
Received in revised form
28 January 2013
Accepted 28 January 2013
Available online 16 February 2013

Keywords:
Scintillation detectors
Ce-doped crystals
Nonproportionality
Fast timing
SiPMs light readout

ABSTRACT

Performance of cerium-doped $Gd_3Al_2Ga_3O_{12}$ (GAGG:Ce) scintillator in gamma-ray spectrometry has been investigated. The measurements of two samples of GAGG:Ce cover the tests of emission spectra (maximum of emission at about 530 nm), light output, non-proportionality, energy resolution, time resolution and decay time of light pulses. We compare the results with commonly known scintillators, such as NaI(Tl), LSO, LuAG etc. The results show that GAGG:Ce has a high light yield of about 33000 ph/MeV as measured with Hamamatsu S3590–18 Si PiN photodiode [1]. The total energy resolution for 662 keV gamma-rays from ^{137}Cs source is equal to about 6%, whereas intrinsic resolution is equal to 5.2%. Additionally, we made basic measurements of photoelectron yield, non-proportionality and total energy resolution of small sample ($5 \times 5 \times 5$ mm^3) of GAGG:Ce crystal coupled to Hamamatsu MPPC array (6×6 mm^2). The results show that the performance of GAGG:Ce measured with the MPPC array are similar to those measured with the PMT.

1. Introduction

Single crystal scintillators with high density and high gamma-ray absorption coefficient coupled with photodetectors are commonly used for detection of high-energy photons and particles. There is continuous demand for new scintillator materials for such application as: X-ray computed tomography (CT), positron emission tomography (PET) and other medical imaging techniques, as well as in high energy and nuclear physics. In the case of modern scintillators, the high light yield, good energy resolution, high effective atomic number, fast scintillation response, chemical stability and capability of large crystal growth are very important parameters. Recently, the best combination of these factors is achieved by Cerium-activated materials, such as silicates, LSO:Ce [2], [3] or LYSO:Ce [4]. They have been developed as promising scintillators for PET due to high density (7.4 g/cm^3 for LSO:Ce and 7.1 g/cm^3 for LYSO:Ce), high effective atomic number (66 for LSO:Ce and 65 for LYSO:Ce), fast decay time (around 35 ns for both scintillators) and high light yield. Also cerium-activated lanthanum halides, such as $LaBr_3$:Ce [5] and $LaCl_3$:Ce [6] reveal very good energy resolution, fast emission and excellent temperature and linearity characteristics.

Oxide materials based on garnet structure are promising candidates as scintillators, because of well mastered technology developed for laser hosts and other applications and easy doping by rare-earth elements, such as lutetium or yttrium. Ce-doped $Y_3Al_5O_{12}$ (YAG:Ce) single crystal was reported in the literature as a fast oxide scintillator [7,8]. Its density is 4.56 g/cm^3 and effective atomic number is 35. The emission spectrum is around 540 nm caused by radiative transmission of Ce^{3+} ions, which is suitable for semiconductor-based photodetectors. Ce- and Pr- doped $Lu_3Al_5O_{12}$ (LuAG:Ce (Pr)) [9–11] single crystals were a subject of study in last decade due to its higher than YAG:Ce density (6.67 g/cm^3) and higher effective atomic number (58.9). Nevertheless, the degradation of light yield and timing properties is observed both in YAG:Ce and LuAG:Ce, because of the Y_{Al} and Lu_{Al} antisite defects (Y and Lu cations localized in octahedral sites of the Al cations) [12]. Such defects create trapping centers and the emission centers in near-UV region. It has been reported that Ga admixture in LuAG hosts can make the energy transfer to Ce^{3+} (or Pr^{3+}) emission centers faster and more efficient that results in higher light yield. However, in these scintillators (for gallium concentrations higher than 20%), Ce^{3+} 5d–4f luminescence is quenched, because of the positioning of 5d states of Ce^{3+} in the

* Corresponding author. Tel.: +48 22 718 0440.
E-mail address: j.iwanowska@ncbj.gov.pl (J. Iwanowska).

0168-9002/$ - see front matter © 2013 Elsevier B.V. All rights reserved.
http://dx.doi.org/10.1016/j.nima.2013.01.064

host conduction band. Further studies shown that an admixture of Gd or La cations can limit the unwanted $5d_1$ state ionization in the Ga-rich garnets [13].

The recent discovery of single crystal multicomponent garnet scintillators, based on YAG crystal with admixture of Ga and Gd, presented by Cherepy et al. [14] and Kamada et al. [15] provide new structures with higher density and effective atomic number.

In this paper, the scintillation properties of new garnet composition: Ce-doped $Gd_3Al_2Ga_3O_{12}$ (Gadolinium Aluminum Gallium Garnet, further named as GAGG:Ce) were characterized. It is a solid, non-hygroscopic single crystal with yellowish color. It is heavy (density ≈ 6.5 g/cm^3), comparable to LSO, YAG or LuAG, which are commonly used for high energy gamma-ray measurements. GAGG:Ce, similarly to those crystals is characterized by high gamma-ray absorption coefficient. Furthermore, it doesn't have any radioactive elements in its structure. The emission maximum for GAGG:Ce is at around 530 nm, which is typical for garnet compositions, and suitable for silicon-based photodetectors. It is characterized by a high light output, above 40000 ph/MeV and a fast decay time constant of the light pulse around of 100 ns, according to [15].

The tests of GAGG:Ce scintillator covered the measurements of emission spectra, decay times, light output in terms of number of photoelectrons per energy unit, non-proportionality of the light output, energy resolution and time resolution. Two samples of GAGG:Ce crystal (both $10\times10\times5$ mm^3) further named as M1 and M2, were tested. Moreover, also the tests of $5\times5\times5$ mm^3 crystal with 6×6 mm^2 Hamamatsu MPPC array were carried out.

2. Experimental setup and results

2.1. Emission spectra

In order to measure the emission spectra, we coupled tested GAGG:Ce samples ($10\times10\times5$ mm^3) to a PC-controlled Digikröm CM110 monochromator window and irradiated them with an intense ^{241}Am source (13.7 GBq). On the other side of the monochromator a calibrated XP2020Q PMT, working in the single photon counting mode, was placed. Light from the tested scintillators was diffracted by a grating system of the monochromator and collected by the PMT. The PMT anode signal was amplified by CAEN N978 fast amplifier and single photoelectron pulses were registered with Ortec 994 multiscaler. The accuracy of the monochromator is ±0.2 nm with 1200 grids per millimeter grating. The spectra (see, Fig. 1) were collected in room temperature (RT). We see the asymmetric emission band that can be fitted in a good approximation with double-Gaussian functions with centroids at 520 nm and 550 nm, respectively. This effect is typically seen in garnet compositions, and can be ascribed to the transitions from the lowest 5d level to the two ground stated $^2F_{5/2}$ and $^2F_{7/2}$ of the Ce^{3+} ions. The energy gap between these states due to spin-coupling was estimated as approximately 2000 cm^{-1}, which corresponds to 256 meV [16]. We also observe a weak emission band around 300 nm, which is connected with 4f–4f transition in Gd^{3+}. Moreover, we see the second order reflection of the monochromator's grating at $\sim$260 nm.

2.2. Decay times

Decay time constants of the light pulse were calculated on the basis of timing spectra obtained using Bollinger–Thomas single photon method [17,18]. The tested samples were coupled to the Photonis XP5500B PMT with high blue sensitivity (up to 13.7 mA/lmF). On the crystal surface a ^{137}Cs gamma-ray source (661.7 keV gamma-ray energy) was taped in order to excite the GAGG:Ce scintillator. Single photons were detected by a fast R5320 Hamamatsu PMT, which is characterized by time jitter of 140 ps, so the time resolution of the prompt time spectrum of timing system, well below 500 ps, was negligible. Each sample was wrapped only on sides with Teflon tape with front surface opened to the Hamamatsu PMT in order to assure the detection of single photons from the scintillator induced by gamma-ray source. The Hamamatsu PMT was placed opposite to the XP5500B PMT at a distance of about 20 cm to assure a single photon detection in R5320 PMT. It requires a detection of less than 2% of events accepted in the tested scintillator. The anode signals from both PMTs were triggering the Philips Scientific constant fraction discriminator (CFD). The time difference between the signals from two PMTs was measured using an Ortec 566 time-to-amplitude converter (TAC). The measurements were gated using two Ortec 551 timing single channel analyzers (SCA) by choosing events with energies corresponding to a full energy peak of 662 keV gamma-rays detected in the XP5500B PMT (the start signal) and a single photoelectron peak detected in the R5320 PMT (the stop signal). The calibration of decay time spectra was performed by using an Ortec 462 time calibrator.

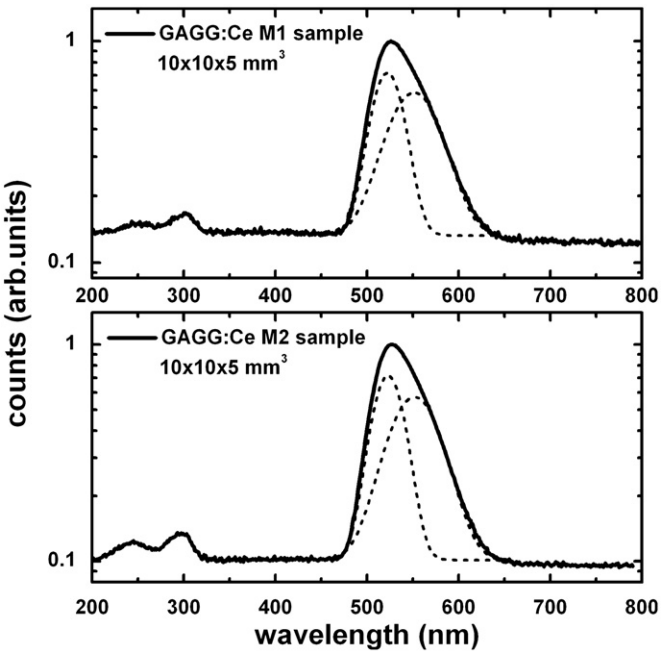

Fig. 1. Normalized emission spectra of GAGG:Ce samples measured with calibrated XP2020Q Photonis PMT. The results were corrected for the quantum efficiency of the PMT and for the spectral response of the grating system.

The results of the measurements were fitted by double-exponential curves in OriginPro 8.6 [19] software

$$y = A_1 e^{-x/\tau_1} + A_2 e^{-x/\tau_2} + y_0 \quad (1)$$

where A_1, A_2 are the amplitudes of the curves, τ_1 and τ_2 are the components of the decay time, y_0 is the baseline offset originating of random coincidences, which contribution was determined in the region before the light pulse. We also calculated the intensity of these components from the equations:

$$I_1 = \frac{A_1\tau_1}{A_1\tau_1 + A_2\tau_2} \quad \text{and} \quad I_2 = \frac{A_2\tau_2}{A_1\tau_1 + A_2\tau_2}. \quad (2)$$

Decay time spectra for M1 and M2 GAGG:Ce samples together with fits of exponential decay curves are seen in Fig. 2. We observe two components: fast τ_1 is equal to about 127 ns (±6 ns) for the M1 sample and 115 ns (±5 ns) for the M2 one (with intensity I_1 and of approximately 85% for both samples) and the

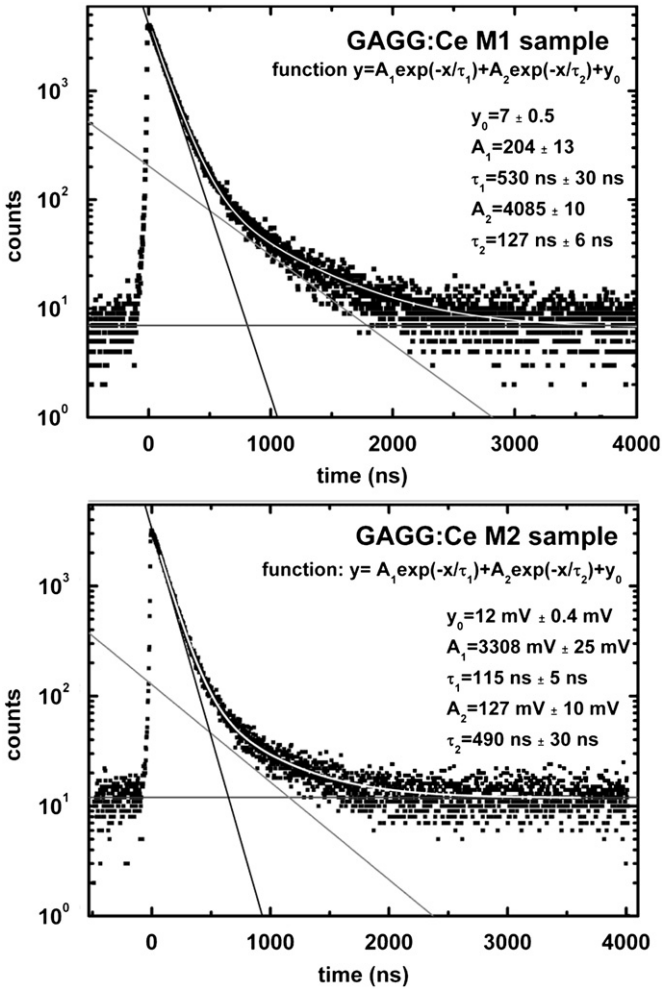

Fig. 2. Light pulse shapes of M1 and M2 GAGG:Ce sample.

second component τ_2 is slow—about 530 ns ($\pm$30 ns) for the M1 sample and 490 ns ($\pm$30 ns) for the M2 one (with intensity I_2 about 15% for both samples). The results obtained for two samples are similar in the range of standard error.

The measured values of decay times differ significantly of that reported in [15]. However, the light pulse shape and its decay time constants were measured by the single photon method, which is the most accurate for the time range below, let to say 200 ns [17]. The observed difference is significant and cannot be accounted, for example to the less accurate scope method used in [15]. Thus it can be related to the fact that the GAGG:Ce is still in the development phase and we cannot exclude different characteristics of particular samples.

2.3. Photoelectron yield and light output

The number of photoelectrons for M1 and M2 samples was determined by means of a single photoelectron method [20,21]. In this method the number of photoelectrons is measured by comparing the position of the full energy peak of γ-rays detected in the crystal to the position of the single photoelectron peak. The samples were coupled to Photonis XP5500B PMT (operating voltage=−1000 V). Additionally, we measured the number of electron–hole pairs with these samples coupled to a Hamamatsu S3590–18 Si PiN photodiode (operating voltage 70 V). We used the ^{241}Am source with energy of 59.5 keV to calibrate the Si PiN diode [21]. It allowed also estimating the light output of the tested samples, based on the typical quantum efficiency characteristic provided by Hamamatsu and the peak emission of the GAGG:Ce crystals. The results are shown in Table 1. The GAGG:Ce is characterized by rather high light yield, comparable to LSO crystal [22], higher than GSO and BGO [23].

The estimated light output is comparable to that of the best LSO crystals [24,25]. However, the results obtained in our measurements differ from those reported by Kamada et al. in [26]. Probably, the discrepancy between both results is caused by the reduced gain in avalanche photodiode (APD) that was used by Kamada et al. The gain of the APD for 5.9 keV X-rays is significantly lower in comparison to that measured for light because of the electric field distortion by charge produced by X-rays in the ionization process. It makes a shift down of the reference X-ray peak, which suggests a larger light output. It was precisely studied in [27] and it was known from earlier study of Hamamatsu APDs by CMS collaboration at CERN [28].

2.4. Non-proportionality of the light output

The non-proportionality of the light yield is defined as a ratio of the photoelectron yield measured for specific gamma-ray energy to that measured for 662 keV from ^{137}Cs source. For non-proportionality measurements radioactive sources covering the energy range of 14.4–1770.2 keV were used (see, Table 2). The measurements were performed for 2 μs shaping time set in the Ortec 672 amplifier. The peaks position (also in the case of escape peaks and double peaks from characteristic X-rays) were determined by Gaussian fit using procedures included in the Multi Channel Analyzer (Tukan 8k) [29].

Fig. 3 presents the non-proportionality characteristics for the tested GAGG:Ce samples coupled to the Photonis XP5500B PMT and for LSO sample coupled to Photonis XP20D0 PMT [30]. The non-proportionality characteristics of the GAGG:Ce samples are similar to LSO in higher energy range and becomes slightly more proportional than LSO for energies below 100 keV, however, essential for its contribution to the intrinsic resolution of scintillators.

Table 1
Basic properties of tested GAGG:Ce samples.

Sample	Photoelectron number (phe/MeV)	Electron–hole pairs number (eh/MeV)	Light output (photons/MeV)
M1	8900 ± 240	29500 ± 450	33100 ± 3000
M2	8200 ± 240	28200 ± 440	31700 ± 3000

Table 2
Radioactive sources used in non-proportionality and energy resolution measurements.

Source	Gamma or X-ray energy (keV)
^{137}Cs	32.2, 661.7
^{133}Ba	31, 81, 276.4, 302.9, 356
^{22}Na	511, 1274.5
^{57}Co	14.4, 122.1
^{60}Co	1173.2, 1332.5
^{65}Zn	1115.6
^{145}Pm	37.4, 67.2
^{109}Cd	22.2, 88
^{54}Mn	834.8
^{207}Bi	75, 569.7, 1063.7, 1770.2
^{241}Am	59.5
^{93}Mo	16.6
^{51}Cr	320.1

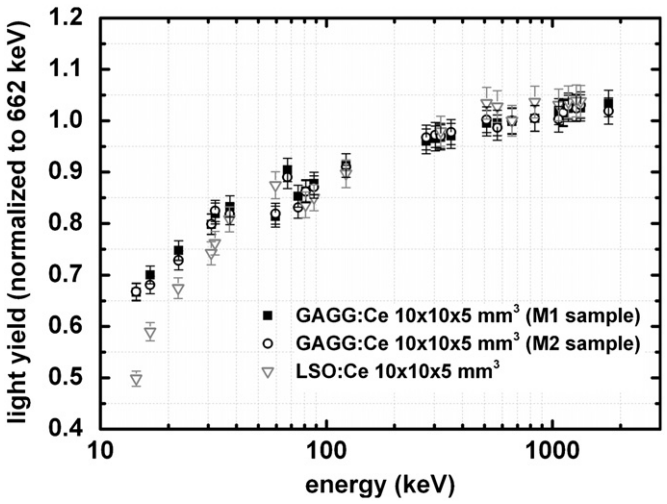

Fig. 3. Non-proportionality characteristics of the tested GAGG:Ce samples and for LSO sample.

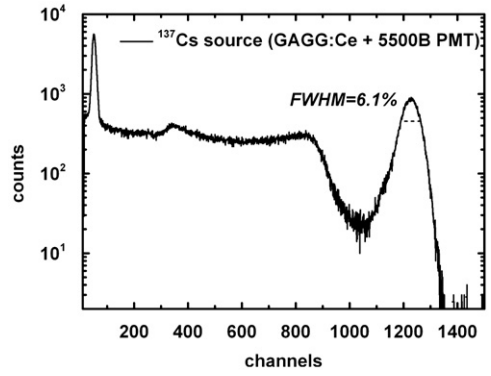

Fig. 4. Pulse height spectrum measured with M1 GAGG:Ce coupled to Photonis 5500B PMT obtained by irradiation with ^{137}Cs source.

2.5. Intrinsic resolution

The energy resolution (ΔE/E) was determined using radioactive sources as described in Table 2. The result for the tested GAGG:Ce scintillators irradiated with 662 keV gamma-rays from ^{137}Cs source is 6.1% for M1 sample and 6.3% for M2 sample, see Fig. 4. The value is much better than those observed with the best LSO crystal [22] and comparable to NaI(Tl) [31].

The total energy resolution of the full energy peak registered with a scintillator coupled to a photodetector can be written as [32]:

$$\Delta E/E = (\delta_{sc})^2 + (\delta_{st})^2 + (\delta_{tr})^2 \quad (3)$$

where δ_{sc} is the intrinsic resolution of the crystal, δ_{st} is the statistical contribution and δ_{tr} is the transfer resolution associated with the variation of light and photoelectron collection. This latter quantity is negligible in modern PMTs [33].

The intrinsic resolution of scintillation crystals is mainly associated with their non-proportional response, but various effects such as inhomogeneities in the crystal structure, impurities or non-perfect reflector covering the crystal may also contribute significantly to overall effect [34].

Assuming Poisson statistics, the statistical uncertainty of the signal from the PMT is described, as:

$$\delta_{st} = 2.35 \times \sqrt{1/N} \times \sqrt{1+\varepsilon} \quad (4)$$

where N is the number of photoelectrons and ε is the variance of the electron multiplier gain, equal to 0.1 for the XP5500B.

Fig. 5 presents the total energy resolution, intrinsic resolution and statistical contribution of tested GAGG:Ce crystals. These scintillators are characterized by a large contribution of intrinsic resolution, following their poor proportionality. However, both these quantities are better than those of $6.02 \pm 0.4\%$ reported for LSO in [22]. The total energy resolution for 662 keV from ^{137}Cs source is equal to $6.1 \pm 0.2\%$ for M1 sample and $6.3 \pm 0.2\%$ for M2 sample, whereas intrinsic resolution is equal to $5.2 \pm 0.1\%$ for both samples.

2.6. Time resolution

Time resolution was measured using experimental set-up described in Fig. 3a in paragraph 2. The test of time resolution was done for 511 keV annihilation quanta from ^{22}Na gamma-ray source. The $10 \times 10 \times 5$ mm^3 GAGG:Ce samples were coupled to a Photonis XP20D0 PMT, characterized by a high blue sensitivity of 13.7 uA/lm [35]. In addition to the time resolution, the number of photoelectrons produced in the PMT by the GAGG crystal was measured. For the reference detector, a truncated cone, 25 mm in diameter and 15 mm high BaF_2 crystal coupled to the XP20Y0Q/DA PMT was used. Its time resolution of 128 ± 4 ps, for 511 keV full energy peak, selected in the side channel, was reported in [36].

The time spectra collected with GAGG:Ce samples are shown in Fig. 6. The results of the measured time resolution are presented in Table 3, in comparison to those measured earlier for LSO, LuAG and $LaBr_3$ scintillators in the same experimental setup [37]. In each case, besides of the time resolution, the number of photoelectrons and decay time constant of the fast component and its relative intensity are listed. Moreover, the timing performances of NaI(Tl) are presented following data of [38], as measured with the XP2020 in the dynode timing mode.

Time resolution measured with GAGG is poorer than those observed with the best Ce and Pr based scintillators, like LSO and LuAG because of a slower decay time of the light pulse. It is, in turn, comparable to those measured with NaI(Tl) and LuAG:Ce crystals. The results are related to much slower light pulses in NaI(Tl) and, in the case of LuAG:Ce, by a weaker intensity of the fast component.

It has been shown in [39] that normalized time resolution – defined as coincidence time resolution multiplied by square root of the number of photoelectrons, measured for 511 keV gamma-rays – is proportional to the square root of the decay time. In order to verify whether the obtained values follow the quoted dependence we have normalized time resolution to the number of photoelectrons and the decay time constant of the fast component, as follows:

$$\frac{\delta_t \sqrt{N}}{\sqrt{\tau}}, \quad (5)$$

where δ_t is the time resolution, N is the number of photoelectrons for 511 keV energy, and τ is the decay time (see, Table 3).

The number of photoelectrons is related to the intensity of the fast component, which determines timing properties. In the sixth column of Table 3, the time resolutions, normalized to the photoelectron number and the decay time constant are listed. It reflects a poorer performance of GAGG related to the slower rise time of the light pulse of 200 ps, reported recently in [40].

2.7. Gamma spectrometry of GAGG:Ce with Hamamatsu MPPC array

The measurements of emission spectra of GAGG:Ce showed that the spectral range of our scintillators is suitable for semiconductor

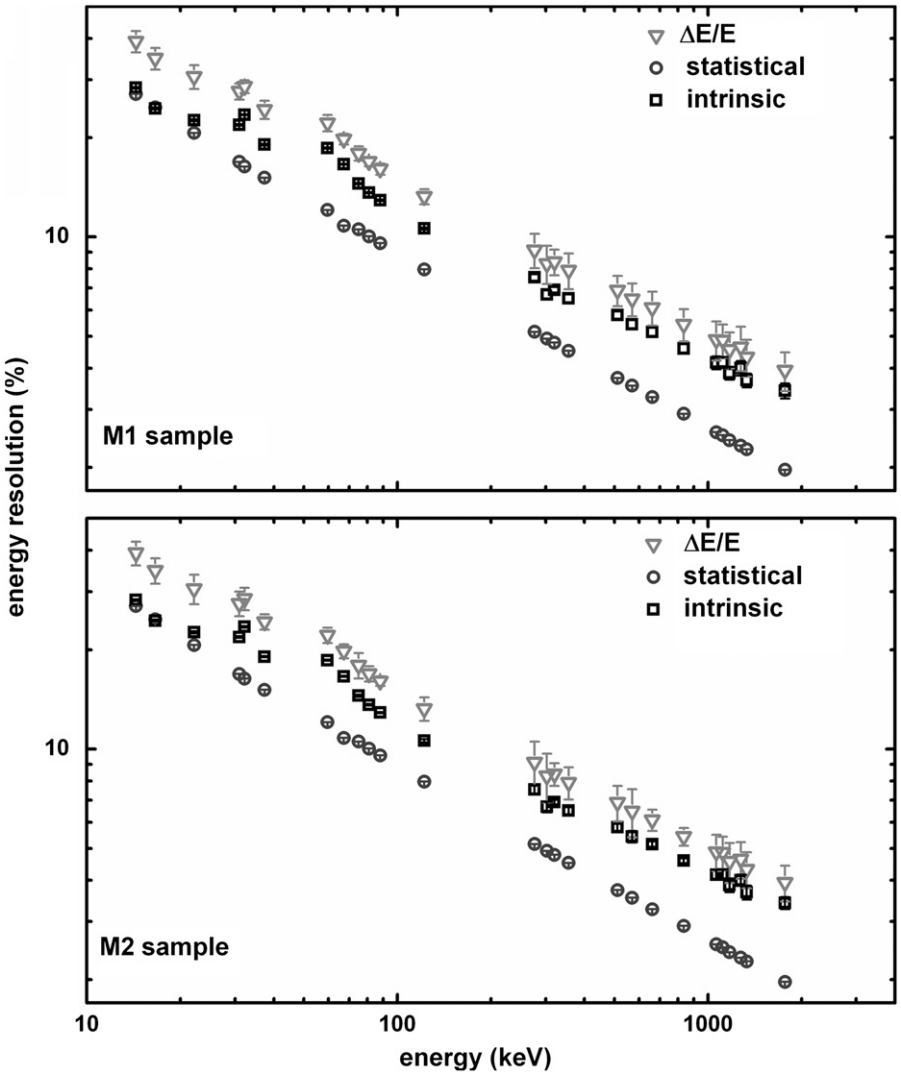

Fig. 5. Energy resolution of tested GAGG:Ce samples (shaping time=2 μs).

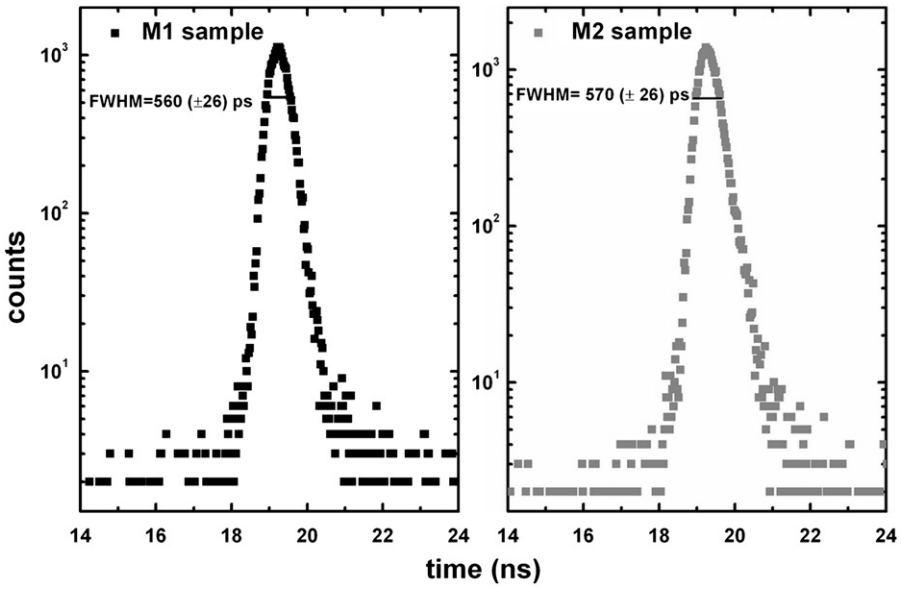

Fig. 6. Time spectra for 511 keV gamma-rays from ^{511}Na source measured with GAGG:Ce crystals coupled to Photonis XP20D0 PMT.

Table 3
Time resolution of GAGG:Ce in comparison to LSO:Ce and LuAG:Pr crystals.

Crystal	Time resolution (ps)	Decay time (ns)	Nphe @ 511 keV	Intensity[b] (%)	$\frac{\delta_\tau\sqrt{N}}{\tau}\times 10^3$	Reference
Ce:GAGG	550 ± 26	133 ± 0.5	2450 ± 120	85 ± 2	2.18 ± 0.34	
Pr:LuAG	308 ± 13	23 ± 2[a]	2860 ± 200	26 ± 2	1.75 ± 0.13	[37]
Ce:LuAG	620 ± 21	69 ± 3	2350 ± 150	23 ± 2	1.72 ± 0.11	[37]
Ce:LSO	166 ± 8	46 ± 2	4400 ± 250	100	1.62 ± 0.10	[37]
Ce:$LaBr_3$	145 ± 13	18 ± 2	11430 ± 400	100	3.7 ± 0.4	[37]
NaI(Tl)	470 ± 18[c]	250	4600 ± 230[d]	100	2.0 ± 0.3	[38]

[a] Mean decay time of the fast components.
[b] Intensity of the fast components relative to entire pulse intensity.
[c] Time resolution measured with XP2020Q in the dynode timing mode.
[d] A typical photoelectron number measured with the XP2020 PMT.

Table 4
Main parameters of MPPC array.

Manufacturer	Hamamatsu
Number of channels	4 (2 × 2 ch)
Active area/channel	3×3 mm^2
Total active area	6×6 mm^2
Number of pixels/channel	14 400
Total number of pixels	57 600
Pixel size	25×25 μm^2
Fill factor	30.8
Gain (at 72.80 V)	2.75×10^5
Spectral range	320–900 nm (maximum sensitivity at 440 nm)
Recomended voltage	72.8 V
Dark count/channel	0.3 Mcps (at 72.8 V)
Capacitance/channel	320 pF

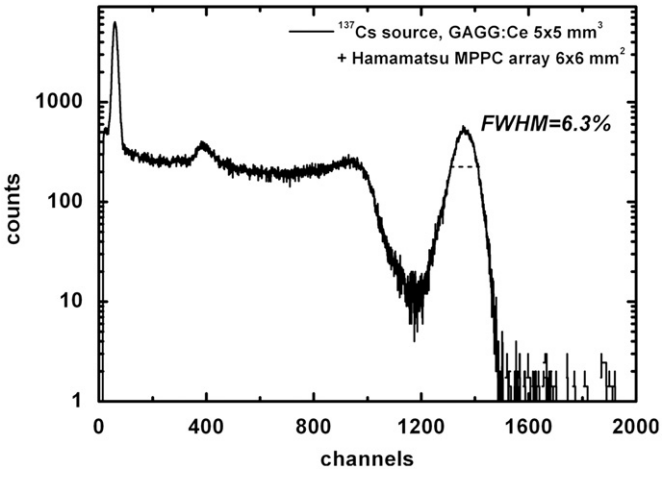

Fig. 7. Pulse height spectrum measured with GAGG:Ce $5\times5\times5$ mm^3 coupled to Hamamatsu MPPC array obtained by irradiation with ^{137}Cs source.

based photodetectors, such as APDs or silicon photomultipliers (SiPM, MPPC). Therefore, we coupled the $5\times5\times5$ mm^3 sample to 6×6 mm^2 Hamamatsu MPPC array. The main parameters of the MPPC array are listed in Table 4. The energy spectrum of ^{137}Cs source obtained with GAGG:Ce coupled to MPPC array is seen in Fig. 7. We can see that results of energy resolution measurements done with MPPC array are similar to those measured with the standard PMT.

We also measured non-proportionality of the light output (see, Fig. 8) and energy resolution (see, Fig. 9) of GAGG:Ce coupled to the MPPC array and compared them to the results obtained with the PMT. We can see that the performance of GAGG:Ce scintillator is similar while measured with the standard PMT and MPPC.

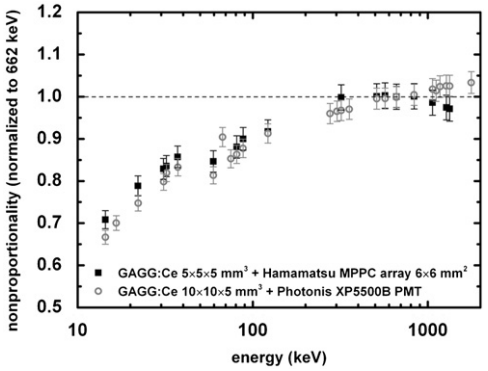

Fig. 8. Non-proportionality curve measured with $5\times5\times5$ mm^3 GAGG:Ce coupled to MPPC array and $10\times10\times5$ mm^3 GAGG:Ce coupled to the PMT.

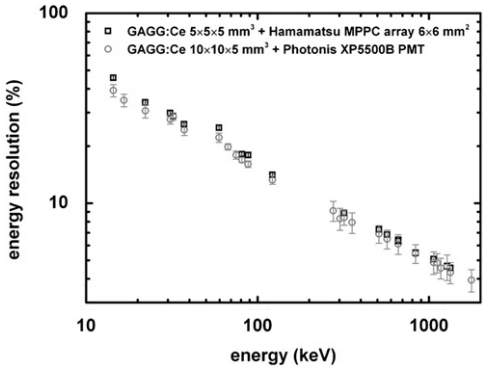

Fig. 9. Energy resolution of GAGG:Ce scintillator measured with two different photodetectors.

In the case of MPPC array we see a decrease in the relative light yield in the energy range above 1 MeV (see, Fig. 10), which is caused by a nonlinear response of MPPC. The linearity of MPPC depends mainly on a total number of APD-cells in a given detector and its effective dead time in relation to the decay time of a scintillator. A nonlinear response for energy higher than 800 keV is the result of too high intensity of scintillator light in relation to the effective dead time of the used MPPC and its total number of APD-cells.

3. Conclusions

The measurements performed with GAGG:Ce scintillator showed that it is characterized by a high light yield, comparable to LSO, larger than BGO and GSO that are commonly used in nuclear medicine, such as CT or PET. The tested samples (both $10\times10\times5$ mm^3) have similar non-proportionality characteristics

as LSO, which is reflected in a comparable energy resolution performance (approximately 6.1% for 661.7 keV energy from ^{137}Cs source). The spectral range of this crystal covers blue and green wavelength, which is more suitable for silicon-based photodetectors rather than for standard PMTs. Time resolution of GAGG:Ce is poorer than LSO (but comparable to commonly known NaI(Tl) crystal), because of longer decay time of the light pulse and a finite rise time of 200 ps. Decay time of the light pulse has two components: fast is about 130 ns and slow – about 500 ns and slightly varies between the samples (they are comparable in the range of systematical error).

We made additional tests with Hamamatsu MPPC array (6×6 mm^2) and small sample of GAGG:Ce ($5 \times 5 \times 5$ mm^3) and obtained similar results to those measured with larger samples coupled to XP 5500B Photonis PMT. The results of decay times obtained with our samples are different than those obtained by Kamada et al. [13,15] probably because the fact that this crystal is still under development. GAGG:Ce appears promising for a wider application in gamma spectrometry.

References

[1] Hamamatsu S3590–18 Si PiN Photodiode Data Sheet 〈http://sales.hamamatsu.com/assets/pdf/parts_S/s3590-08_etc_kpin1052e08.pdf〉.
[2] C.L. Melcher, et al., IEEE Transactions on Nuclear Science NS-39 (1992) 502.
[3] F. Daghighian, et al., IEEE Transactions on Nuclear Science NS-40 (1993) 1045.
[4] D. Cooke, et al., Journal of Applied Physics 88 (2000) 7360.
[5] E.V.D. van Loef, et al., Applied Physics Letters 79 (2001) 1573.
[6] E.V.D. van Loef, et al., IEEE Transactions on Nuclear Science NS-48 (2001) 341.
[7] M. Moszynski, et al., Nuclear Instruments and Methods in Physics Research A 345 (1994) 461.
[8] T. Ludziejewski, et al., Nuclear Instruments and Methods in Physics Research A 389 (1997) 287.
[9] A.G. Petrosyan, et al., Journal of Crystal Growth 312 (2010) 3136.
[10] K. Kamada, et al., Journal of Crystal Growth 352 (2012) 91.
[11] N. Cherepy, et al., Nuclear Instruments and Methods in Physics Research A 579 (2007) 38.
[12] Y. Zorenko, et al., Radiation Measurements 38 (2004) 677.
[13] K. Kamada, et al., Journal of Physics D Applied Physics 44 (2011) 505104.
[14] N. Cherepy et al., Proceedings of SPIE 7079X, (2008), September 04.
[15] K. Kamada, et al., Crystal Growth and Design 11 (2011) 4484–4490.
[16] G.H. Dieke, Spectra and Energy Levels of Rare-Earth Ions in Crystals American Journal of Physics 38(1970) 399, http://dx.doi.org/10.1119/1.1976350.
[17] L.M. Bollinger G.E. Thomas, Review of Scientific Instruments, vol. 32, p. 1044.
[18] M. Moszynski, et al., Nuclear Instruments and Methods in Physics Research 142 (1977) 417.
[19] OriginPro web page: 〈http://www.originlab.com/index.aspx?go=Products/OriginPro〉.
[20] M. Bertolaccini, S. Cova, C. Bussolatti, Proceedings of the Nuclear Electronic Symposium, Versailles, France, 1968.
[21] M. Moszynski, et al., IEEE Transactions on Nuclear Science SN-44 (1997) 1052.
[22] M. Kapusta, et al., IEEE Transactions on Nuclear Science NS-52 (2005) 1098.
[23] M. Moszynski, et al., IEEE Transactions on Nuclear Science NS-54 (2007) 723.
[24] M. Moszynski, et al., IEEE Transactions on Nuclear Science NS-51 (2004) 1074.
[25] M. Moszynski, et al., IEEE Transactions on Nuclear Science NS-57 (2010) 2886.
[26] K. Kamada, et al., IEEE Transactions on Nuclear Science NS-59 (2012) 2112.
[27] M. Moszynski, et al., IEEE Transactions on Nuclear Science NS-48 (2001) 1205.
[28] J. Pansarat, et al., Nuclear Instruments and Methods in Physics Research A 389 (1997) 186.
[29] Tukan 8k Analyzer Data Sheet 〈http://www2.ipj.gov.pl/tukan_en/〉.
[30] M. Grodzicka, et al., Nuclear Instruments and Methods in Physics Research A 652 (2011)226 652 (2011).
[31] L. Swiderski, et al., IEEE Transactions on Nuclear Science NS-54 (2007) 1372.
[32] G.F. Knoll, Radiation Detection and Measurements, 3rd ed., Wiley, New York, 2000.
[33] M. Moszynski. et al., Proceedings of SPIE, 5922 (2005), 1, Article no. 592205.
[34] M. Moszynski, et al., Nuclear Instruments and Methods in Physics Research A 484 (2002) 259.
[35] M. Moszynski, et al., Nuclear Instruments and Methods in Physics Research A 567 (2006) 31.
[36] M. Moszynski, et al., IEEE Transactions on Nuclear Science NS-51 (2004) 1701.
[37] L. Swiderski., et al., IEEE Transactions on Nuclear Science NS-56 (2009) 2499.
[38] B. Bengtson, M. Moszynski, Nuclear Instruments and Methods in Physics Research 204 (1982) 129.
[39] T. Szczesniak, et al., IEEE Transactions on Nuclear Science NS-56 (2009) 173.
[40] J.Y. Yeom et al., Presented at SORMA 2012 Conference.